Bull. of Atmos. Sci.& Technol. (2025) 6:14
https://doi.org/10.1007/s42865-025-00101-5

CASE STUDY

# Study on associated effects of extreme drought and heatwave on air quality in South Africa during october 2022

**Farahnaz Fazel-Rastgar[1,2] · Venkataraman Sivakumar[2] · Masoud Rostami[3,4] · Bijan Fallah[5]**

Received: 27 November 2024 / Accepted: 26 February 2025


**Abstract**
This study investigates the impact of combined drought and extreme heatwave events on air quality in South Africa during October 2022 (study period). An analysis of meteorological data revealed a sharp increase in surface air temperature and a significant decrease in precipitation, resulting in an extreme heatwave and drought period. The Standardized Precipitation Evaporation Index (SPEI) for October 2022 showed an extreme drought value of -2.01, reflecting increased dryness over the past two decades. Meteorological analysis highlighted the influence of the intensified stationary Angola heat low and Botswana upper ridge subtropical high, facilitating dry and warm air advection into the region, exacerbating an extreme climatic situation with heatwave conditions. Ozone levels exceeded 80 ppb (unhealthy) in northern, central, and eastern regions, particularly on October 13, with concentrations ranging between 88.2 and 93 ppb. Long-term data (1980–2022) showed rising trends in PM2.5 and black carbon concentrations, peaking at $1.48 \times 10^{-8}$ kg/m³ and $8 \times 10^{-10}$ kg/m³ in October 2022, with the highest values in Free State Province. Additionally, the UV Aerosol Index (UVAI) showed significant growth over the last decade, with high values in October 2022, signaling worsening air quality and environmental health concerns. The findings emphasize the important need for mitigation measures to address the compounding effects of extreme weather on air quality and public health.

**Keywords** Air quality · Climate extreme · Drought · Heatwave · South Africa

✉ Farahnaz Fazel-Rastgar
farah_rast@yahoo.com

[1] School of Chemistry and Physics, University of KwaZulu Natal, Durban 4000, South Africa

[2] S. V. Raman Researchers Roadmap, Westville, Durban 4000, South Africa

[3] Potsdam Institute for Climate Impact Research (PIK), Potsdam, Germany

[4] Laboratoire de Météorologie Dynamique (LMD), Sorbonne University (SU), Ecole Normale Supérieure (ENS), Paris, France

[5] German Climate Computing Center (DKRZ), Hamburg, Germany

Published online: 19 March 2025

## 1 Introduction

Drought is a gradual and often silent phenomenon caused by prolonged precipitation shortages over extended periods, typically spanning months or even seasons. Its effects, though slow to emerge, are extensive and deeply felt across sectors such as agriculture, society, economics, and the environment, impacting communities worldwide (Edwards et al. 20142018; Zhao and Running 2010). Human life has historically faced various natural threats, many of which are driven by climatic factors that vary by region (Ebi et al. 2021; Talley et al. 2021; Thomas et al. 2018; Falkner and Buzan 2022; Weckroth and Ala-Mantila 2022). Anomalies in meteorological trends, such as rainfall and temperature, are key drivers of atmospheric disturbances (Richard et al. 2001; Ge et al. 2021; Qian et al. 2023; Zhang et al. 2023). These fluctuations, especially in regions like southern Africa, pose serious challenges to ecosystems (Anderegg and Anderegg 2013, 2014; Greenwood et al. 2017; Sankaran Greenwood et al. 2019). Additionally, seasonal forecasting systems predict climate variables such as precipitation and temperature months in advance, helping to assess drought risk. These forecasts aid in early warning and preparation, especially in drought-prone regions, by providing insights into potential water shortages and climate shifts (Arnone et al. 2020). Moreover, the bias correction method can improve the prediction of extreme temperature values, although fewer ensemble members identified rainfall extremes, highlighting a challenge due to limited data on extreme events (Trentini et al. 2022).

Water scarcity is a clear symptom of climatic shifts affecting many arid and semi-arid areas, which cover approximately 66% of Africa (Okello et al. 2024). This continent, the world's second-largest and hottest, faces recurrent drought events of varying intensities every few years (Werner et al. 2015; Mwale and Gan 2005). Water is essential for sustaining ecosystems and biodiversity, yet droughts can lead to significant ecological and environmental degradation. Future water demand is expected to increase as the population grows and social needs change, intensifying the risk of water scarcity, particularly during dry periods. Notably, drought impacts vary across climates, including in South Africa. Droughts are often prolonged, lasting for months or even years, with severe events leading to crop failures and cattle mortality, as seen in the southern African drought of 1991–1992, which caused a loss of nearly three million tons of grain (Sivakumar and Hansen 2007; Dilley and Heyman 1995).

The relationship between droughts and heatwaves has garnered significant attention due to their devastating effects on ecosystems, agriculture, and public health (Mukherjee et al. 2020; Qian et al. 2023). The African continent has experienced increasingly frequent extreme weather events, such as heatwaves, droughts, and floods, over recent decades (Russo et al. 2016; Odoulami et al. 2017; Fazel-Rastgar and Sivakumar 2022, 2024; Meque et al. 2022). Research indicates that heatwaves have become more common in Africa, particularly in the past 20 to 30 years (Ceccherini et al. 2017). In South Africa, heatwaves are projected to increase by over 3.5 times under current climate scenarios (Lyon 2009). A recent study shows that the average maximum temperatures may increase by up to 6 °C over much of South Africa by 2070–2099 (Mbokodo et al. 2020). Future climate analysis indicates a rise in heatwave events, with the most significant increases (80–87%) predicted to occur during the summer months (Kapwata et al. 2022). The southern region of Africa endured some of its most severe droughts during the summer, especially over 2015–2016 (Russo et al. 2016; Yuan et al. 2018; Mbokodo et al. 2020; Onyeuwaoma et al. 2024). Given the socioeconomic

challenges associated with compound heatwaves and droughts in southern Africa, there is an urgent need for comprehensive studies to understand these complex events.

Drought can also drive chronic pollution, with heatwaves accelerating pollutant release over short periods and intensifying air quality degradation. Clean air is vital for human and environmental health (Nolte et al. 2018). In the United States, for example, climate change is anticipated to worsen air quality by increasing harmful contaminants like low-level ozone and particulate matter from drought-stricken or wildfire-affected areas (Nolte et al. 2018). A recent study observed that PM10 concentrations increased by 26.7–46.7% during dry periods (Šmejkalová and Brzezina 2022). It is estimated that over 90% of air pollution-related deaths occur in low- and middle-income countries, particularly in Asia and Africa. Wildfire risks increase during drought, contributing to particulate matter, such as PM2.5, in the atmosphere (Guan et al. 2020). In the western United States, wildfire frequency is projected to increase, largely due to rising temperatures and water deficits (Abatzoglou and Williams 2016). Similarly, PM2.5 associated with wildfires has been increasing in the northwestern United States (McClure and Jaffe 2018).

Ozone pollution also poses risks to public health and ecosystems. Drought influences surface ozone through meteorological and vegetation responses (Lei et al. 2022). While some plants absorb low-level ozone through their stomata, others emit volatile organic compounds (VOCs) that react with atmospheric chemicals to produce ozone (Vivaldo et al. 2017; Llusià et al. 2002). Dry conditions can raise ozone levels, as plants close their stomata to conserve water, reducing their ability to filter pollutants. Efforts to limit nitrogen oxide (NOx) emissions, which react with VOCs to form ozone, are critical, as drought-induced VOC increases can offset the benefits of reduced NOx levels (Demetillo et al. 2019). In West Africa, poor air quality is driven by anthropogenic sources, such as transportation, industries, and waste combustion, as well as natural biogenic emissions. Coastal regions experience significant pollution from shipping, offshore oil and gas operations, and dense populations, leading to increasing health risks as urbanization and industrialization grow.

In southern Africa, the Botswana High's intensification during drought creates warmer, drier conditions as subsiding air warms adiabatically (Reason 2016; Driver and Reason 2017; Blamey et al. 2018). Additionally, intense winds during droughts can lift dust particles from dry soils, contributing to poor air quality (Attiya and Jones 2022; Al Ameri et al. 2019; McTainsh et al. 2005; McTainsh et al. 1989). Recent studies using neural network analysis have indicated that drought prediction in South Africa is quite complicated and varies with different meteorological parameters, including significant local variability (Onyeuwaoma et al. 2024). Droughts can also lead to electricity disruptions by reducing the availability of hydropower, which, in turn, forces reliance on fossil fuels, increasing emissions and air pollution, thereby escalating the social costs associated with climate change (Qiu et al. 2023).

Specific weather patterns, such as stable atmospheric conditions like temperature inversions, cold high-pressure systems, or prolonged dry periods, can worsen air pollution by trapping pollutants close to the surface, affecting air quality. Additionally, weather patterns significantly influence air pollution levels, which can lead to health issues such as respiratory diseases, as seen during the COVID-19 pandemic (Fazel-Rastgar and Sivakumar 2023). Climate change is increasing heatwaves, which in turn enhances ozone pollution (Wang et al. 2024). High temperatures and sunlight accelerate ozone formation, while stagnant air traps pollutants, worsening air quality (Wang et al. 2023).

Comprehensive drought risk assessment is essential for macro-level planning, sustainable development, natural resource management, and fostering resilient human-environment interactions. This study aims to investigate the compound impacts of drought and extreme heatwaves on air quality in South Africa during October 2022.

## 2 Material and data collection

This study analyzed meteorological datasets, including temperature, humidity, and pressure, from the National Centers for Environmental Prediction (NCEP) and the National Center for Atmospheric Research (NCAR). The NCEP-NCAR reanalysis utilizes a state-of-the-art analysis and forecasting system (Kalnay et al. 1996a, b) with a spatial resolution of 2.5°X 2.5° and global (Lat/Lon) grid coverage at 144° X 73° points. This reanalysis method incorporates data assimilation from 1948 to the present. For this study, October monthly mean composites and anomalies were examined, with anomalies calculated as the monthly average departure from the climate normal (1991–2020), providing a baseline for long-term climate change analysis.

October 2022 monthly mean precipitation data over the study area were sourced from the Global Precipitation Climatology Centre (GPCC) v2020 dataset (Rustemeier et al. 2021; Schneider et al. 2016, 2017). The GPCC has monitored precipitation since 1982, with data quality controlled from approximately 7,000 stations. The full data product (V2020) spans from the year 1891 to 2019, based on quality-checked input data from 67,200 stations globally, and includes records of 10 years or more. This dataset provides accumulated monthly values on a square grid with spatial resolutions of 0.25° × 0.25°, 0.5° × 0.5°, 1.0° × 1.0°, and 2.5° × 2.5° latitude/longitude. Precipitation anomalies across all stations are interpolated and overlaid on the GPCC Climatology V2011 data. Additionally, the most recent data, interpolated to a 1°x1° grid, cover stations examined since 2020. GPCC climatological assessments address systematic gauge errors and include the total number of gauges used per grid.

Maximum and minimum observational data for the Durban meteorological station in 2022 were obtained from Iowa State University of Science and Technology, with some values calculated based on reported hourly data, representing actual maximum and minimum values for the period observed. Furthermore, the October monthly and daily mean values of various atmospheric contaminants were derived from NASA's Modern-Era Retrospective Analysis for Research and Applications (MERRA) database (Rienecker et al. 2011). Data for the standardized precipitation evaporation index (SPEI) were obtained from the SPEI Global Database (https://spei.csic.es/database.html). The SPEI is an extension of the standardized precipitation index (SPI), which accounts for both precipitation and potential evaporation (PET) to assess drought (Vicente-Serrano et al. 2010). The SPEI provides a scale for both positive and negative values, identifying wet and dry events and representing water balance (precipitation minus PET). Common parameterizations for PET include the Penman-Monteith and Thornthwaite equations, which use primary variables such as humidity, wind speed, available energy, and air temperature. Unlike the SPI, the SPEI can capture the impact of elevated temperatures on water demand. According to classifications from Soulé (1992) and Paulo et al. (2012) for SPEI drought classes, there are five categories: no drought (SPEI > -0.5), mild drought (SPEI between −0.5 and −1), moderate drought

(SPEI between −1 and −1.5), severe drought (SPEI between −1.5 and −2), and extreme drought (SPEI < -2). The SPEI can be calculated on various time scales, ranging from 1 to 48 months. Mean temperature data are taken from the NOAA NCEP CPC 0.5°x0.5° Global Daily Gridded Temperature, while monthly precipitation data are obtained from the Global Precipitation Climatology Centre (GPCC). The CPC data, with a 0.5°x0.5° resolution, are interpolated to one degree. Here, data are sourced from the Global SPEI database, which provides robust, long-term global drought information with a one-degree spatial and monthly resolution, based on monthly precipitation and potential evapotranspiration values (https://spei.csic.es/database.html).

In this study, we used the heatwave threshold baseline map for South Africa provided by the South African Weather Service (SAWS) (https://www.weathersa.co.za/home/weatherques). SAWS defines a heatwave as occurring when the maximum temperature in a specific town exceeds 5 °C above the average maximum temperature of the hottest month for that area, lasting for three or more consecutive days. More details, including a comprehensive map of the heatwave threshold, can be found on the SAWS website (https://www.weathersa.co.za/home/weatherques). Also, the extreme drought was identified using the Standardized Precipitation Evaporation Index (SPEI) with values below −2. Also, linear regression was used for trend analysis to determine the relationship between a dependent variable and time.

Here, for the validation, comparing the datasets with long-term historical trends and patterns, confirms whether the data is consistent with known climate variability and past events.

The present study is focused over South Africa and geographical map is illustrated in Fig 1.

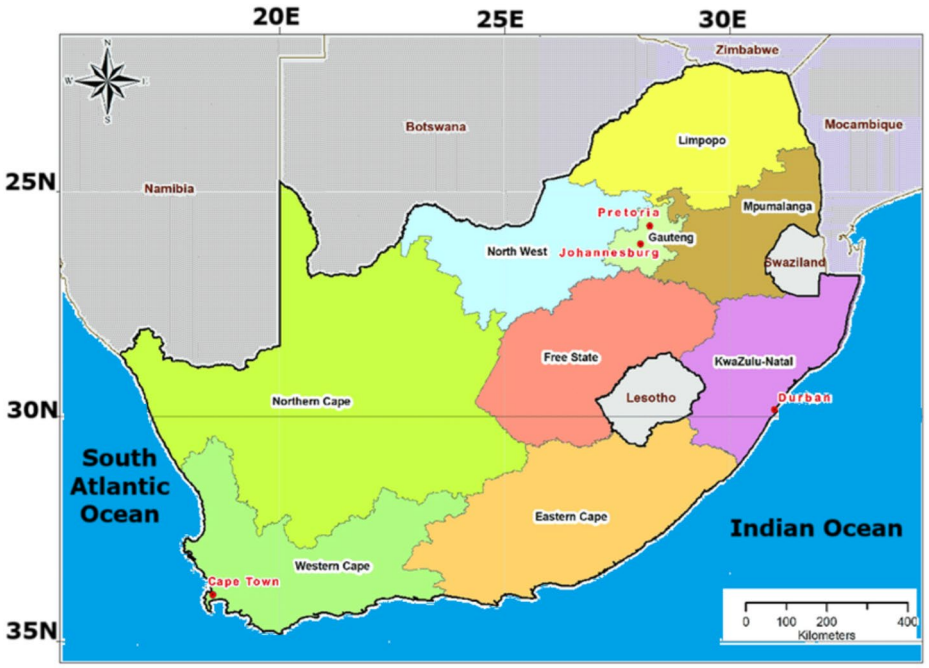


**Fig. 1** Geographical map of South Africa, highlighting its provinces and borders

# 3 Results

## 3.1 Temporal variations in surface temperature and precipitation over the study area

The long-term variations in surface air temperature and October precipitation rates over the study area are presented in Fig. 2a and b. These long-term data show a positive temperature trend with a significant peak of approximately 22.2 °C in 2022, alongside a negative precipitation trend. Data were obtained from the NCEP-NCAR reanalysis for October and area-averaged over −35.2° to -21.9°S and 16.9° to 33.8°E from 1948 to 2022. This trend reflects warmer atmospheric surface temperatures with decreased precipitation, particularly over the past decade. Figure 2c and d display the long-term deviations shown in Fig. 2a and b, respectively. Figure 2a and b reveal a marked increase in October 2022 surface air temperature by a maximum of 2.232 °C and a precipitation decrease of -0.22 mm/day in the study area. These series reveal an extreme heat event for October 2022, accompanied by reduced precipitation across the study area.

In these analyses, a paired samples t-test was performed to examine the change in surface air temperature and precipitation rate from 1948 to 2022. The test yielded a p-value of $p < 0.00001$, strongly suggesting statistically significant changes in both surface air temperature and precipitation rate. Figure 3a provides a composite anomaly map of precipitation (mm) for October 2022, with data from the Global Precipitation Climatology Centre (GPCC) v2020 dataset. The anomalies are calculated relative to the 1991–2020 period. This figure shows that most of the study area experienced a precipitation deficit ranging from 5 to 40 mm, although some southern Free State, northern Eastern Cape, and KwaZulu Natal areas show increases between 5 and 20 mm. A maximum increase of approximately 20 mm was observed primarily in northwestern Limpopo Province during the heat event. Figure 3b displays surface potential evaporation anomalies ($Wm^{-2}$) over the study area, indicating a substantial increase, especially in Limpopo Province (exceeding 90 $Wm^{-2}$). However, in parts of Mpumalanga and KwaZulu Natal, surface potential evaporation decreased (nega-

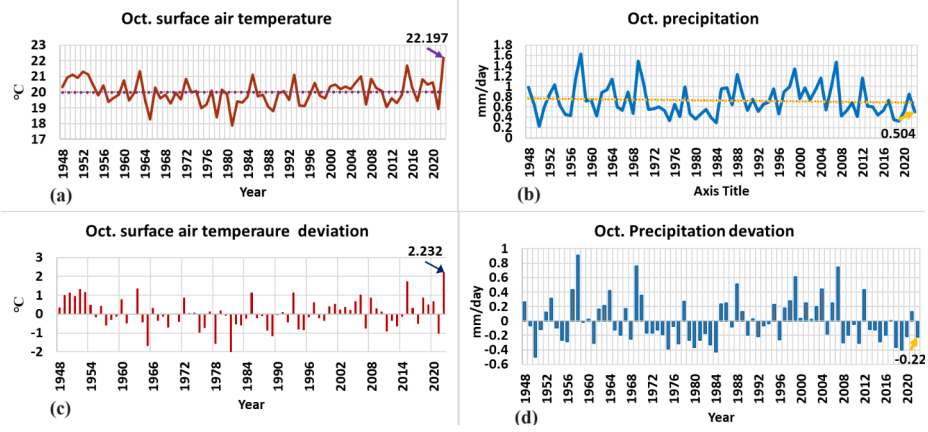


**Fig. 2** Long-term temporal variations in (**a**) surface air temperature, (**b**) precipitation rate, (**c**) deviation of surface air temperature, and (**d**) deviation of precipitation rate over the study area for October from 1948 to 2022

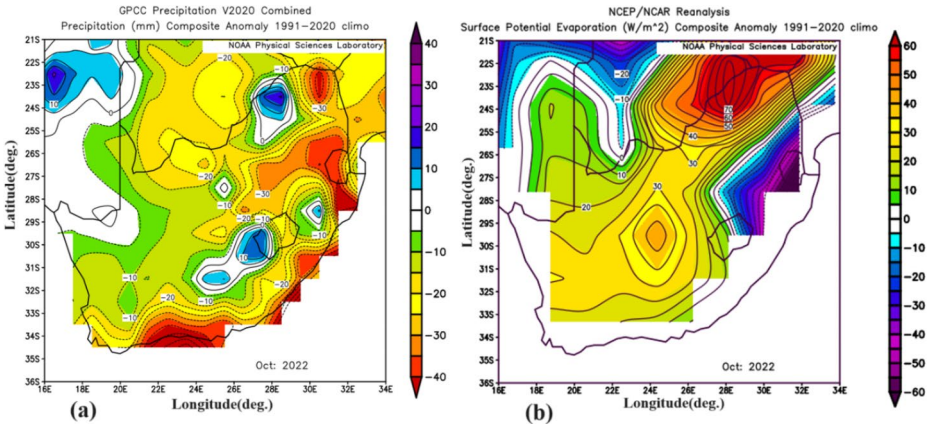


**Fig. 3** Anomalies in precipitation (**a**) and surface potential evaporation (**b**) for October 2022 in the study area

tive values in anomaly). Central and western areas also show increased evaporation beyond (positive values in anomaly) climate-normal values, associated with high surface air temperatures during the October 2022 heatwave.

Figure 4a shows the surface air temperature anomaly map for October 2022, with anomalies ranging from 1.5 to 3.5 °C, peaking in Northern Cape Province. Figure 4b is a Hovmöller diagram, obtained from the MERRA-2 (Rienecker et al. 2011) database, showing the maximum daily 2 m temperature over the study area for October 2022. This diagram highlights extreme heat events on October 2, 9, 11, and 13, with a later event on the 30th, predominantly affecting western South Africa. Additional reanalysis from NCEP-NCAR for daily maximum temperatures shows abnormally high values, peaking at 7.5 K, primarily during the first 13 days (not shown here). Durban in KwaZulu Natal was selected as an example of an October 2022 heatwave in South Africa. Figure 4c displays the daily maximum and minimum observational temperature data series for Durban's meteorological station in 2022, obtained from Iowa State University of Science and Technology (https://mesonet.agron.iastate.edu/request/daily.phtml), with some values based on reported hourly data. This figure shows a peak maximum temperature of 35 °C on October 13, 2022 (indicated by a yellow arrow). The yearly maximum temperature deviation analysis reveals a peak 10.33 °C higher than the 2022 mean temperature for that date (Fig. 4d). The South African Weather Service issued a media release on October 4, 2022, noting an unusually warm October. This study, therefore, explores the synoptic and dynamic aspects of October 2022.

### 3.2 Standardized precipitation evaporation index (SPEI)

Figure 5a shows a time series for the SPEI area averaged over South Africa during October from 1990 to 2022, illustrating an increase in drought over the study area during the past two decades for month of Octobre. This figure clearly indicates significant values in 2015 (the lowest value of -2.5) and the years 2019 (-2.1) and 2022 (-2.01), which correspond to extreme droughts over the past decade.

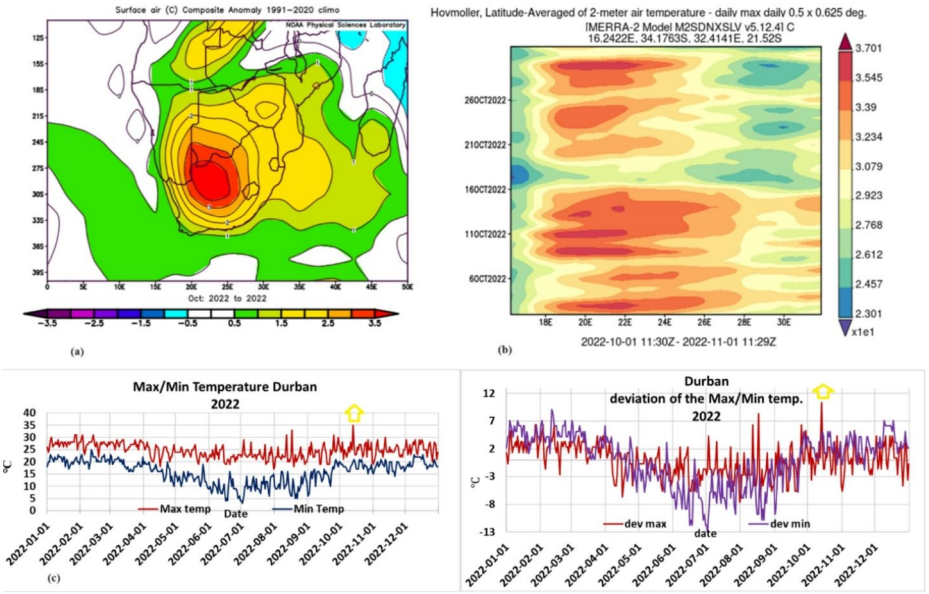


**Fig. 4** Surface air temperature anomalies (**a**) and Hovmöller diagrams (**b**) obtained from the MERRA-2 database. Time series of the maximum and minimum observational temperature data for the Durban meteorological station during 2022 (**c**), and time series for the deviations of the maximum and minimum observational temperature data (**d**) for the Durban meteorological station during 2022

In these analyses, a paired samples t-test was performed to examine changes in South Africa from October 1990 to 2022, illustrating an increase in drought over the study area in the past two decades. The test yielded a p-value of $p < 0.00001$, suggesting statistically significant changes. The SPEI was area-averaged over the study area to assess these changes.

Figure 5b displays the standardized precipitation evaporation index (SPEI) for South Africa during October 2022 (https://spei.csic.es/database.html). This figure highlights extreme drought conditions (with SPEI values below −2) primarily over the western part of South Africa, southern Namibia, and parts of Botswana, Zimbabwe, and Mozambique in October 2022.

### 3.3 Weather maps analysis of the heatwave case

Figure 6 shows charts for the mean sea pressure (MSLP) composite mean (a), MSLP climate normal (b), and MSLP anomalies (c) for October 2022 over the study region. This composite mean map illustrates the development of the Angola thermal low-level heat low pressure (centered southeast of Angola at 1011 hpa) trough, which extended from the northern boundaries to the study area. Figure 6b presents a climate normal map (departure 1991–2020) of the sea level pressure over the study area, showing a rather weaker pattern of heat low. However, as Fig. 6c indicates, during the study period, the thermal low-pressure trough intensified mainly in the western areas, reaching a maximum of approximately 15 hPa in the western Cape Province. In southern Africa, the heat low forms over Angola (~14°S) in September and October due to intense surface heating. As the Southern Hemisphere enters summer (November to March), the heat lows shift southward, forming over

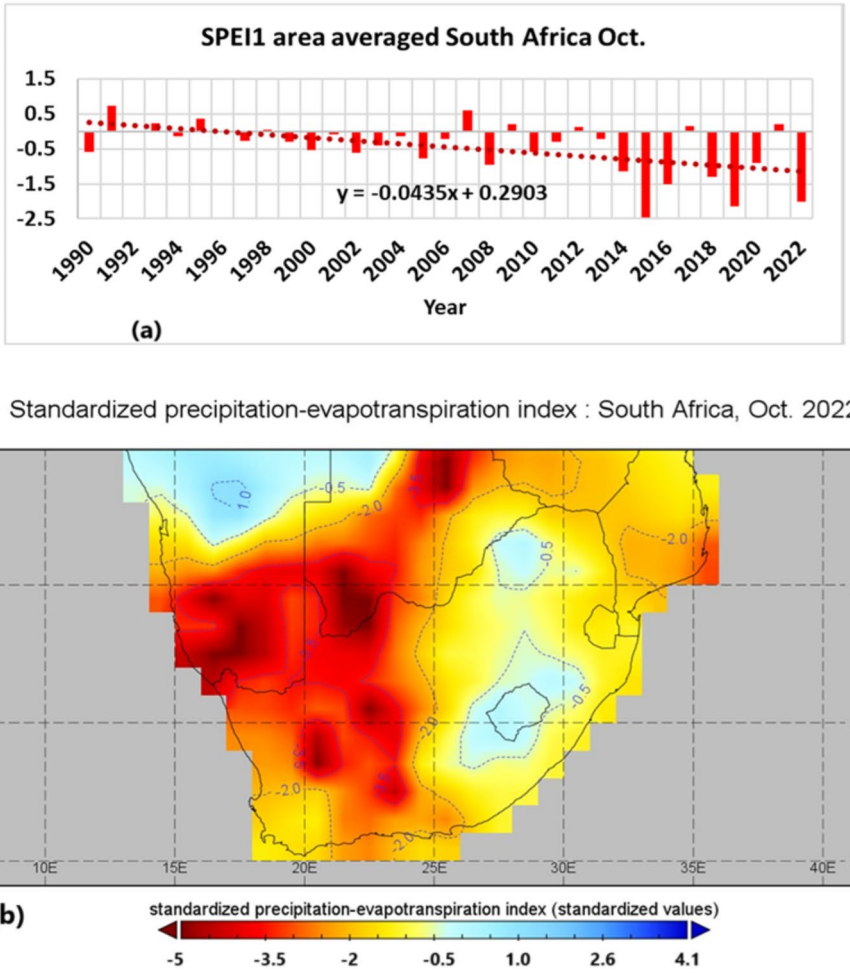


**Fig. 5** Time series for the SPEI area averaged over South Africa during October from 1990–2022 (**a**), and the SPEI over South Africa during October in 2022 (**b**)

Namibia (~20°–26°S), driven by the dry, desert conditions. These low-pressure zones affect local winds, suppress rainfall, and can influence tropical systems in the region (Attwood et al. 2024).

The mid-tropospheric geopotential height map at 500 hPa (Fig. 6d) shows the existence of the subtropical Botswana high, centered over Botswana, with a closed contour of 5895 gpm. The general pattern of the climate normal map for Fig. 6d, presented in Fig. 6e, demonstrates a weaker subtropical high over the southern African countries. However, during the study period, the subtropical ridge intensified, with a maximum increase of 45 gpm, primarily over parts of the Free State, Western Cape, Eastern Cape, and KwaZulu-Natal provinces (Fig. 6f). The anomaly map for 500 hPa for October 2022 (Fig. 6f) displays an abnormally intensified penetration of the subtropical Botswana high system, which shifted southward into the study area. This shift is associated with a relatively warmer situation

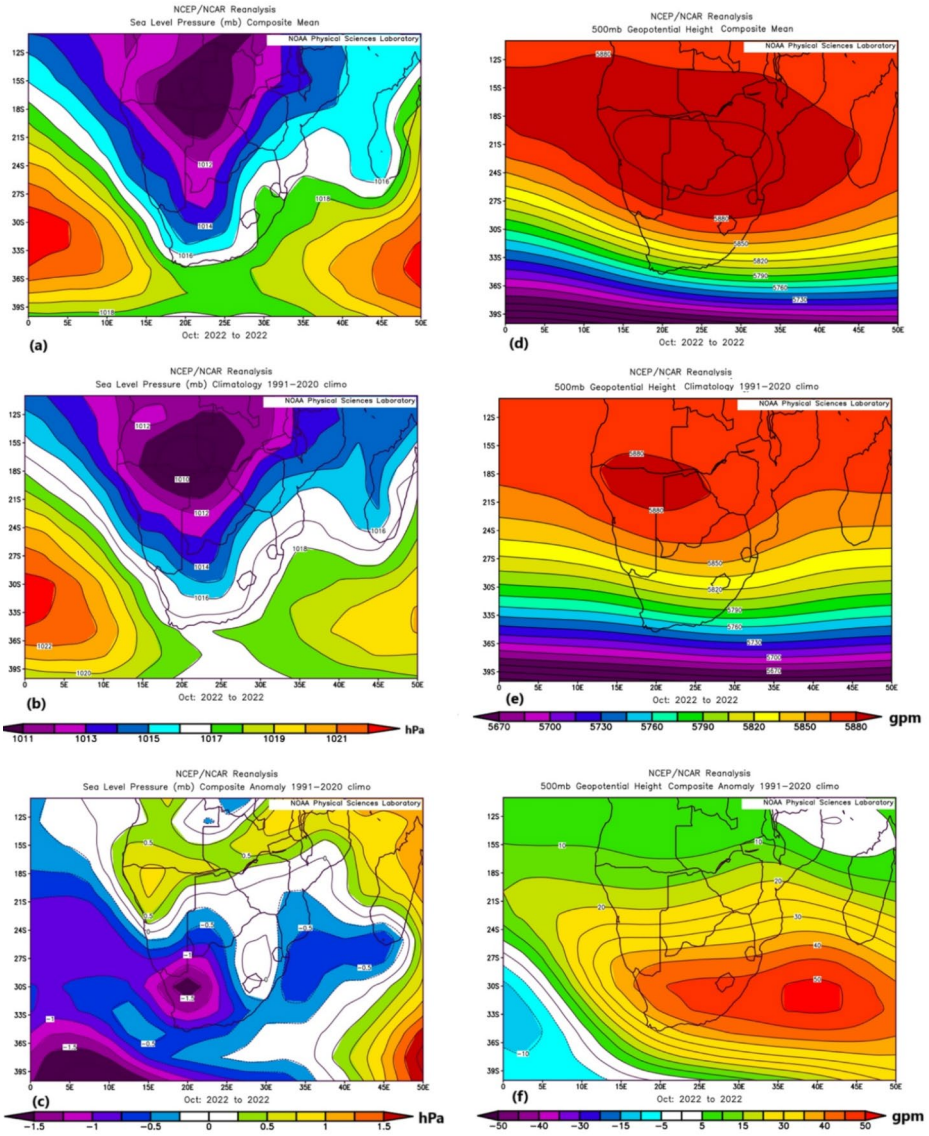


**Fig. 6** Mean sea pressure (MSLP) composite mean (**a**), MSLP climate normal (**b**), MSLP anomalies, 500 hPa composite mean (**d**), 500 hPa climate normal (**e**), and 500 hPa anomalies maps during October 2022 over the study region

(see Fig. 7), leading to the occurrence of a heatwave in the study area. The mid-tropospheric Botswana subtropical high-pressure system typically forms in August and strengthens as it moves southward over southern Africa during the austral spring and summer months. It plays a significant role in shaping rainfall and temperature patterns in the region. As the Botswana High strengthens, it tends to bring dry, cooler conditions to the southern parts of the continent, suppressing rainfall and leading to warmer temperatures. This system's

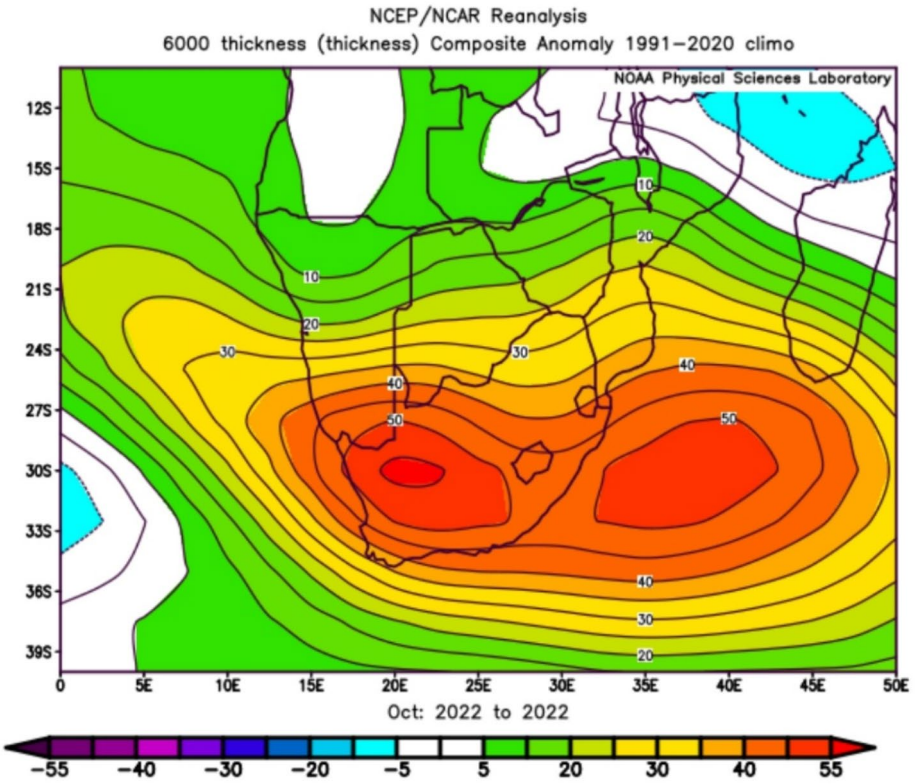


**Fig. 7** Anomaly map of the thickness between 1000 and 500 hPa for the study area during the study period

position and strength influence the overall climate, including the distribution and intensity of rainfall, especially during the dry months, and its interaction with other systems like the Angola Low affects the seasonal variations in both rainfall and temperature (Driver and Reason 2017).

Additionally, the anomaly map of the thickness (1000−500 hPa) reveals greater thicknesses ranging from 25 to 55 gpm across all parts of the study area. This is linked to an abnormally warm air column that dominated the area in October 2022 (Fig. 7). Therefore, the analysis of low- and mid-level tropospheric maps illustrates the southward shift of the more intensified Angola thermal low-level heat low-pressure trough toward the study area. This has been coupled with an abnormal and intensified system of Botswana's high compared to the normal climate pattern. Thus, the low- and mid-level tropospheric structure patterns reveal the development of an abnormal intensity of the Botswana high over the study area.

During the summer in the Southern Hemisphere, the Angola Low is a non-dynamical thermal low pressure associated with strong surface heating (Munday and Washington 2017). The Angola heat low is characterized by an area of low surface pressure, positioned between 16–20°S and 18–22°E, as indicated in the climate mean from the beginning of austral spring (October). In austral spring, the Angola low acts as a thermal heat low, formed

in response to the high surface temperatures in the Angola region (Munday and Washington 2017).

In general, thermal lows can develop near sea level pressure during the warm season, especially in summer, due to strong heating compared to their surrounding areas. Intense solar heating over the land surface leads to warming in the lower levels of the atmosphere. Because hot low-level air is less dense than colder, denser air, a low-pressure system will develop and rise faster in height than in the surrounding atmosphere, maintaining the same altitude.

The vertical cross-sections of the relative humidity composite mean and surface soil moisture anomalies over the study area during the heatwave of October 2022 are presented in Fig. 8(a) and 8(b). These figures demonstrate dry conditions over the study area during the heatwave. Additionally, vertical cross-sections of air temperature along with their anomalies are shown in Fig. 8(c) and 8(d), respectively. A comparison of the mean and anomalies in the vertical pattern of air temperatures over the study area reveals anomalously warm air, primarily in the low and mid-tropospheric levels. However, at upper levels, around 300 − 100 hPa (near the jet stream level), an opposite structure with colder air formed during

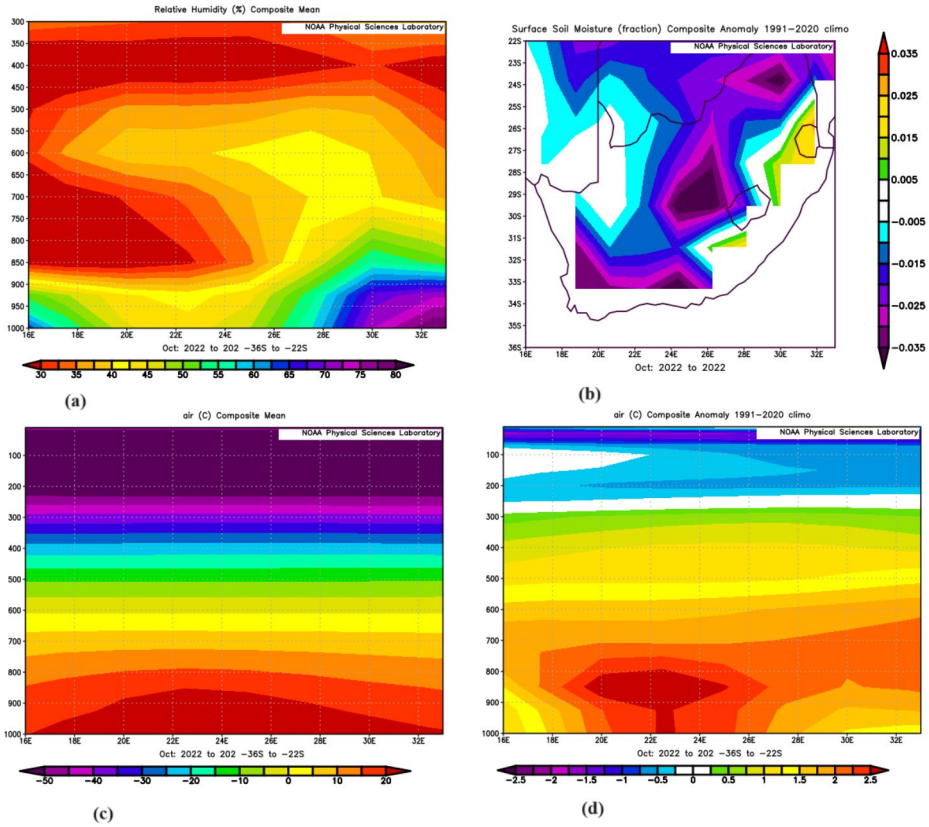


**Fig. 8** Relative humidity composite mean (**a**), surface soil moisture (**b**), vertical cross-section composite mean of the air temperature, (**c**) vertical cross-section composite mean of the air temperature anomalies (**d**) over the study area during the heatwave in October 2022

the study period. This is correlated with relatively stable cold conditions at the jet stream level and strong subsidence, leading to increased surface temperatures.

Based on Fig. 8(b), lower soil moisture than normal can be associated with dryness over agricultural and vegetated lands in South Africa. These areas can experience low soil moisture and groundwater levels, along with increased evaporative stress (Fig. 3c) during the study period. Consequently, with persistently warmer temperatures compared to normal values, drought can become more widespread over longer periods, as indicated by the SPEI (see Fig. 5).

The wind vector analysis at the surface (Fig. 9a) reveals warm (Fig. 9b) and dry (Fig. 9c) currents from northern countries such as Mozambique, Zimbabwe, Botswana, and desert areas, predominantly affecting the northern Cape Province and central South Africa. Dry winds are often associated with drought, leading to the advection of dry and hot air masses from continental regions into the study area. North-easterly and north-westerly winds prevail in the study area, exhibiting a high daily frequency (October monthly analysis) with dry, warm air. This is associated with a stationary thermal heat low that causes northerly dry-hot currents into the study area, which developed during the warm season (see Fig. 6a).

Thus, dry and warm flows from northern areas between the northerly thermal low northwest and anticyclonic ridges reach the southwest (Atlantic Ocean) and southeastern (Indian Ocean) boundaries (Fig. 9a). However, only the southern marine boundaries are influenced by cold and humid air masses associated with temperature and humidity gradients, resulting in unstable weather conditions during October 2022.

The upper-level wind vectors at 200 hPa are presented in Fig. 10a. The anomalies for Fig. 10a show the intensification of northward flows coming from warmer latitudes compared to long-term mean values over the study area. The anomaly maps for upper tropospheric (200 hPa) zonal and meridional winds reveal a weakening of the westerlies (except in some small southern areas) and southerly currents toward the study area during the extreme heat event (figures are not presented here).

The vertical cross-sections of the relative humidity composite mean and surface soil moisture anomalies over the study area during the heatwave of October 2022 are presented in Fig. 8 (a and b). These figures demonstrate the dryness conditions over the study area during the heatwave in October 2022. Additionally, the vertical cross sections of the air temperature along with its anomalies are shown in Fig. 8c and d, respectively. A comparison of the mean and anomalies in the vertical pattern of the air temperatures over the study area reveals anomalously warm air, mostly over low and mid-tropospheric levels. However, in the upper level at approximately $300-100$ hPa (at around the level of jet stream), the opposite structure associated with colder air formed during the study period. This is correlated with relatively stable cold conditions around the level of the jet stream and strong subsidence, increasing the surface temperature. Based on Fig. 8b, lower soil moisture rather than normal can be associated with dryness over the agricultural and vegetation lands in South Africa. These areas can suffer from low soil moisture and groundwater levels along with an increase in evaporative stress (Fig. 3c) for the mentioned study time. Therefore, with persistently abnormal warmer temperatures rather than normal values, drought can be more widespread over longer periods in the SPEI (see Fig. 5).

The surface wind vector analysis (Fig. 9a) revealed warm (Fig. 9b) and dry (Fig. 9c) currents from northern countries such as Mozambique, Zimbabwe, Botswana, and desert areas, mostly to the northern Cape Province and central South Africa. Dry winds can mostly

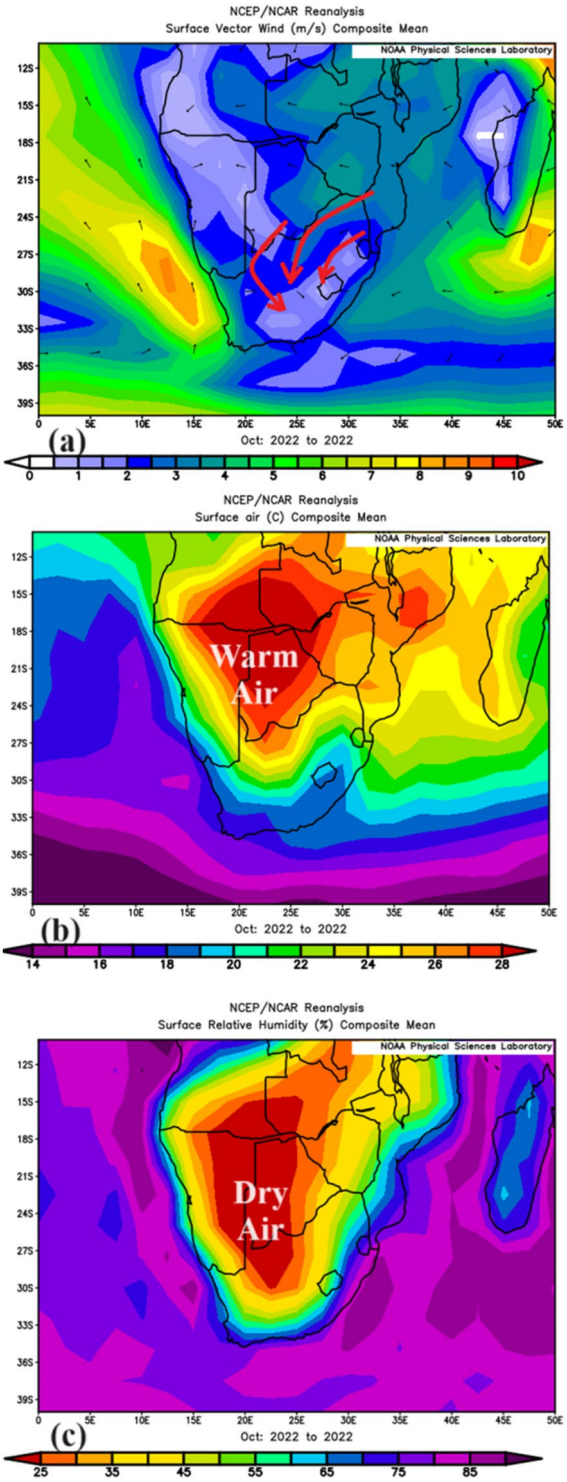


**Fig. 9** Surface wind vector (**a**), surface air temperature (**b**), and surface relative humidity (**c**) over the study area for October 2022

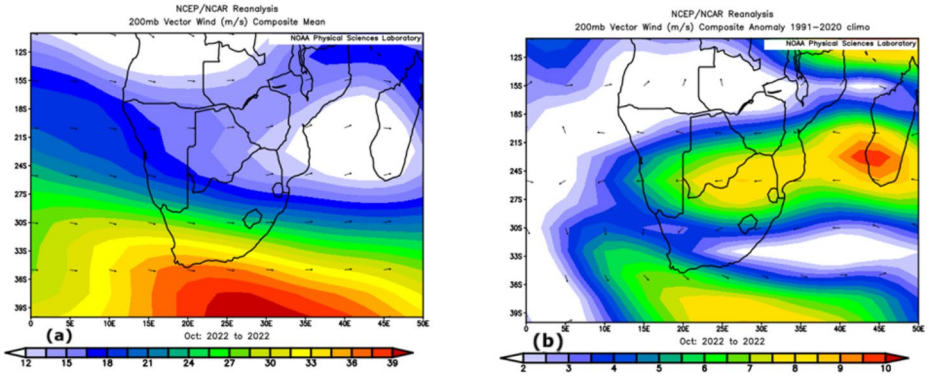


**Fig. 10** 200 hPa wind vectors composite mean (**a**) and 200 hPa wind vector anomalies (**b**) during the study period over the study area

be accompanied by drought and cause the advection of dry and hot air masses from continental areas to the study area. The surface north easterly and northwesterly winds prevail in the study area and have a high daily frequency (October monthly analysis) with dry warm winds. This is associated with a stationary thermal heat low (causing northerly dry-hot currents into the study area), which developed during the warm season (see Fig. 6a). Therefore, dry and warm flows from the northern areas between the northerly thermal low northwest and anticyclonic ridges reach the southwest (Atlantic Ocean) and southeastern (Indian Ocean) boundaries (Fig. 9a). However, only the southern marine boundaries are affected by cold and humid air masses associated with temperature and humidity gradients, resulting in unstable weather activities during October 2022. The upper-level wind vectors at 200 hPa is presented in Fig. 10a. The anomalies of the wind vectors at 200 hPa (Fig. 10b) display the intensification of north flows coming from warmer latitudes rather than long-term mean values over the study area. The anomaly maps for upper tropospheric (200 hPa) zonal and meridional winds reveal weakening of the westerlies (except some small areas in the south parts) and southerly currents toward the study area during the extreme heat event (figures are not presented here).

### 3.4 Air quality observations

The high-resolution maps obtained from the MERRA-2 database illustrate the low-level daily average ozone mass mixing ratio over South Africa on specific days (October 2, 9, 11, 13, and 29, 2022) during the extreme heat days (see Fig. 3b) were analyzed (all figures are not presented here). The results reveal high ozone levels exceeding 80 ppb (considered unhealthy) specifically on October 13, across the study area, primarily affecting the northern, central, and eastern regions. Figure 11 indicates elevated low-level ozone concentrations in northeastern North Cape, North West Province, and southern Free State Province, ranging from 88.2 to 93 ppb.

Additionally, Fig. 12a presents a yearly time series of the low-level ozone mass mixing ratio obtained from the MERRA-2 database, averaged over the study area from October 2004 to 2022. This figure illustrates a very slight positive trend in ozone levels over the past three decades. However, this figure clearly shows a significant maximum value of 75.9 ppb

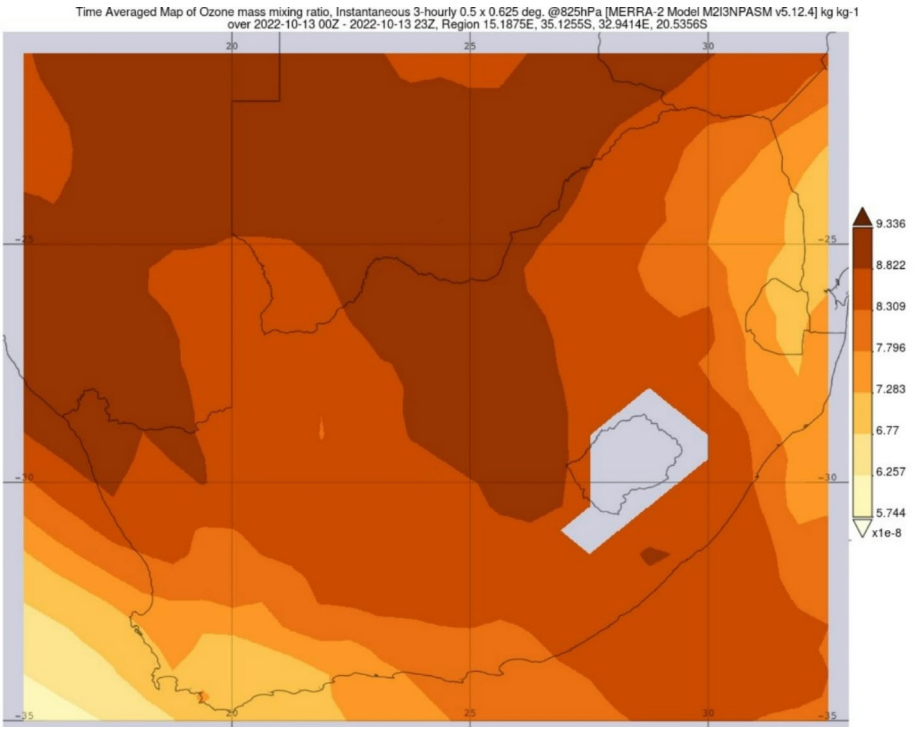


**Fig. 11** Low-level daily average data for the ozone mass mixing ratio over South Africa on October 13, 2022

recorded during the study period in comparison with other years. This increase is associated with extreme heatwave events during this timeframe. The figure also shows another significant high value (75.2 ppb) in October 2015, during the study period.

The paired samples t-test for a yearly time series of the low-level ozone mass mixing ratio, obtained from the MERRA-2 database and averaged over the study area from October 2004 to 2022, yielded a p-value of $p < 0.0001$, indicating statistically significant changes in the low-level ozone mass mixing ratio over the study period.

Figure 12b displays a time-averaged distribution map, indicating higher values (~80–84 ppb) predominantly in the northwestern province during the study period.

Figure 13a shows the area average of a long-term time series (1980–2022) for the total mass concentration of PM2.5 at the surface over the study area, based on datasets obtained from the MERRA-2 database. This figure reveals a positive trend in the surface total mass concentration of PM2.5, peaking at $1.48 \times 10^{-8}$kg m$^{-3}$ in October 2022, corresponding with extreme heatwaves in the region. The paired samples t-test conducted on the annual time series data (1980–2022) for the total mass concentration of PM2.5 at the surface, using datasets from the MERRA-2 database, resulted in a p-value of $< 0.0001$. This indicates a statistically significant change in the PM2.5 concentration over the study period. Figure 13b illustrates the October monthly average of the total mass density column of the long-term PM2.5 time series from 1980 to 2022, indicating a second peak during the study period, with a value of approximately $5 \times 10^{-5}$kg $^{-3}$. Figure 13c presents the October monthly aver-

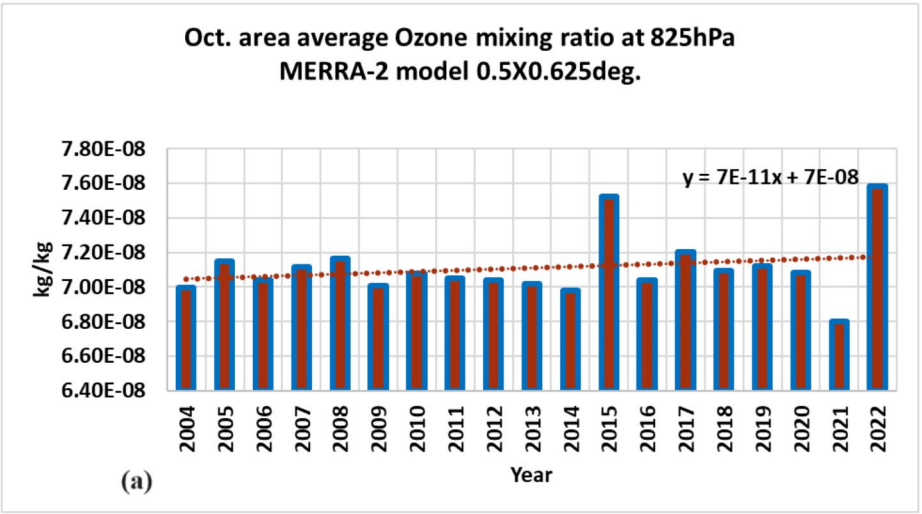


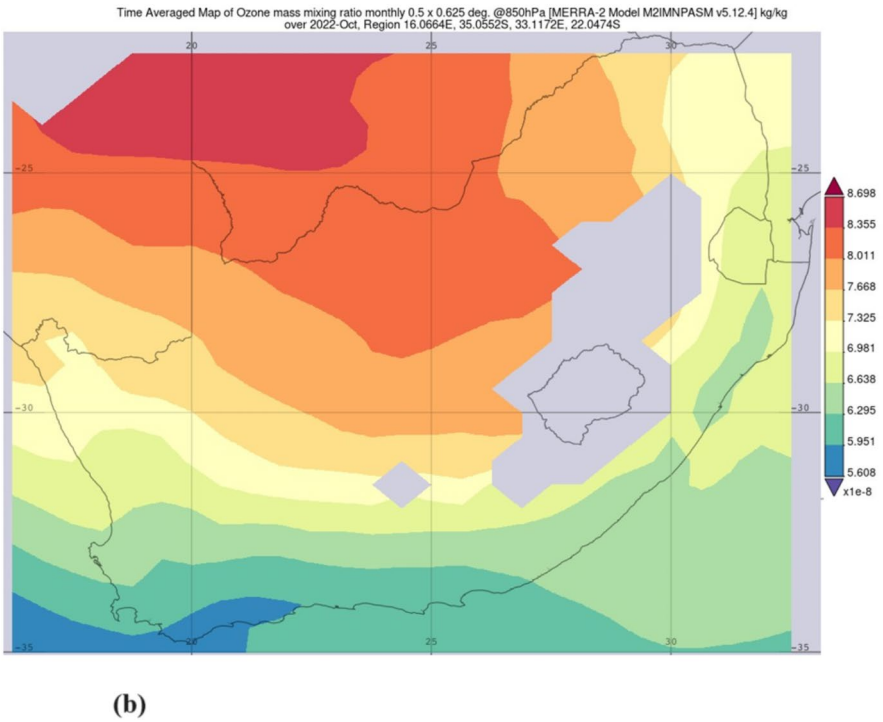


**Fig. 12** Yearly time series of the low-level ozone mass mixing ratio (**a**) for October from 2004 to 2022 and October 2022 time-averaged distribution map of the low-level ozone mass mixing ratio (**b**) over the study area

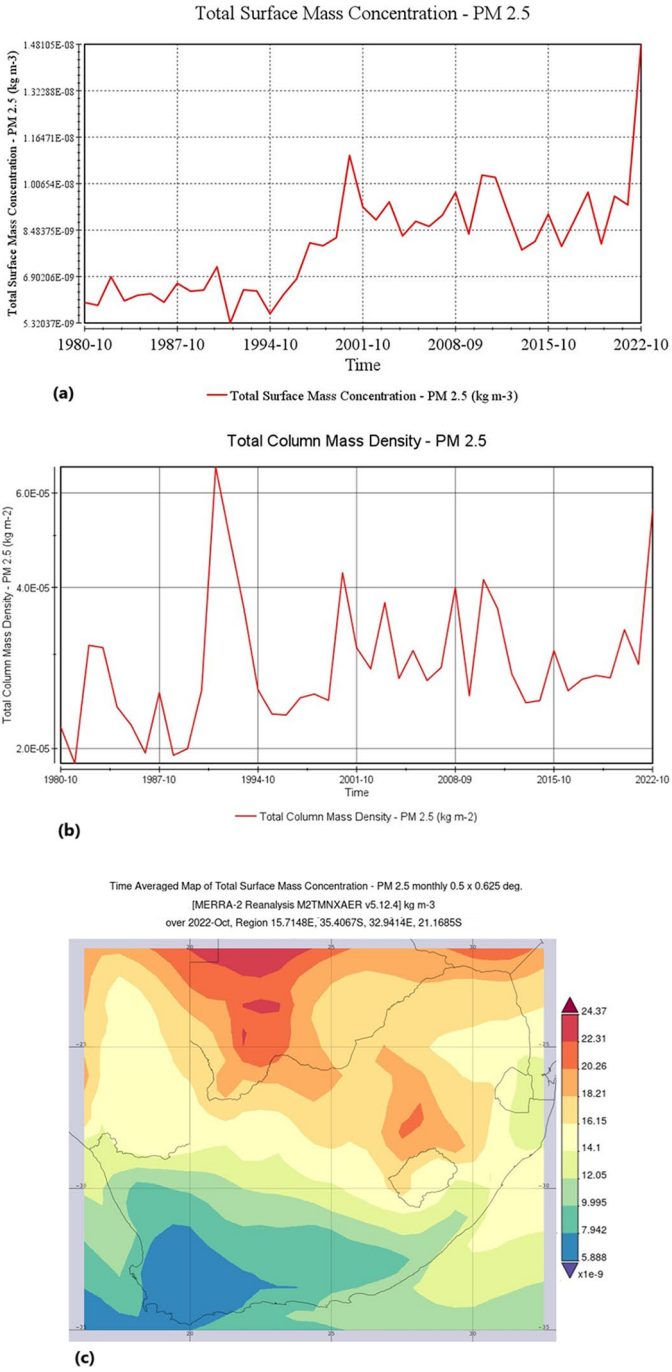


**Fig. 13** Total surface mass concentration of PM2.5 in an area average during 1980–2022 for month of October (**a**), average total mass density of PM2.5 from 1980 to 2022 for the month of October (**b**), and monthly average of surface PM2.5 over the study area (**c**) for month of October in 2022

age PM2.5 levels over the study area in 2022, showing elevated values of approximately 24 kg $m^{-2}$, primarily in the Free State Province. During severe droughts, such as those experienced in the United States between 1990 and 2014 from March to October, mean increases in PM2.5 and surface ozone were reported at 17% (1.6 µg $m^{-3}$) and 8% (3.5 ppb), respectively (Wang et al. 2017).

Figure 14a depicts an area average of a long-term time series (1980–2022) for the black carbon surface mass concentration over the study area, sourced from the MERRA-2 database. This figure shows a sharp positive trend in black carbon surface mass concentration, peaking at $8 \times 10^{-10}$kg $m^{-3}$ in October 2022, which is associated with the extreme heat wave in the region. The paired samples t-test performed on a long-term time series (1980–2022) for the black carbon surface mass concentration over the study area, sourced from the MERRA-2 database, yielded a p-value of $<0.0001$. This indicates statistically significant changes in black carbon concentration over the study period. Figure 14b displays the October monthly average of the total mass density column of black carbon over the same long-term period, indicating a second peak during the study period with a value of approximately $3.81 \times 10^{-6}$kg $m^{-2}$. Figure 14c presents the same air contaminant for the October monthly average over the study area in 2022, revealing high values of approximately $175.2 \times 10^{-11}$ kg $m^{-3}$, primarily concentrated in the Free State and North West provinces.

It is noteworthy that drought can lead to electricity disruptions, such as increased reliance on hydropower and fossil fuel sources, which are associated with higher emissions and air pollution, contributing to the social cost of climate change (Qiu et al. 2023). Figure 15 illustrates a time series (a) and map distribution (b) of the ultraviolet aerosol index (UVAI) averaged over the study area from 2004 to 2022 (data available from 2004). This figure indicates significant growth in UVAI, with high values recorded in October 2022 compared to the previous decade. The map shows higher values in the eastern area including the city of Durban in the KwaZulu Natal province. The Ultraviolet Aerosol Index (UVAI) measures aerosol particles in the atmosphere that can affect UV radiation levels. Aerosols can absorb or scatter UV radiation, influencing exposure. High UVAI values indicate increased aerosol presence, which can impact on health. Monitoring UVAI helps predict UV risks, enabling better health precautions, especially in areas with high pollution or during events like wildfires.

## 4 Discussion and conclusions

This study examined meteorological data and trends in surface temperature and precipitation across South Africa, with a particular focus on the extreme heatwave experienced in October 2022. An analysis of datasets from the NCEP-NCAR reanalysis and the GPCC highlighted a significant increase in surface temperatures, reaching an unprecedented peak of 22.2 °C, while simultaneously noting a decrease in precipitation rates across the region. The observed anomalies revealed a substantial precipitation deficit, particularly in areas affected by the heatwave. The SPEI analysis indicated a concerning rise in drought conditions over the past two decades, underscoring the interplay between elevated temperatures and water scarcity. Weather maps showed the intensified Angola low-pressure system and subtropical Botswana high, contributing to the extreme climatic conditions observed.

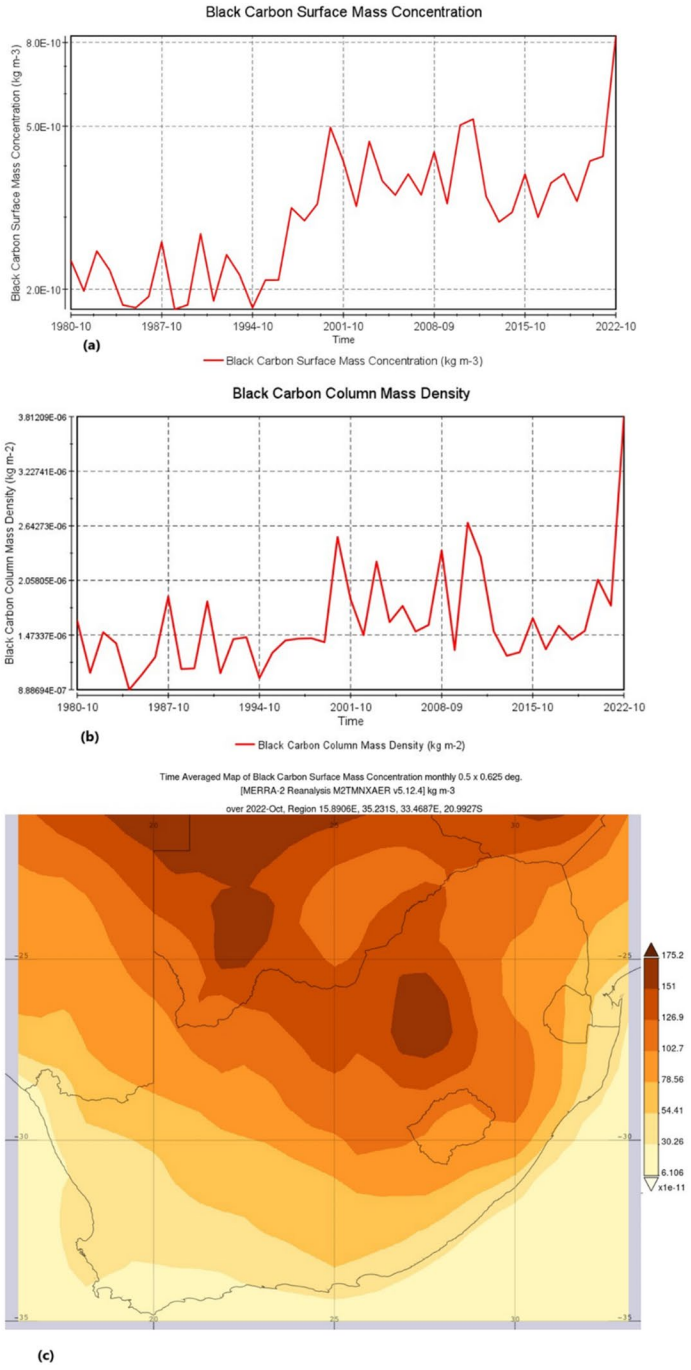


**Fig. 14** (**a**) Total surface mass concentration of black carbon in an area average over October for a long time series from 1980–2022, October monthly average of the total mass density of black carbon (**b**) from 1980 to 2022, and October monthly average of surface black carbon (**c**) over the study area in 2022

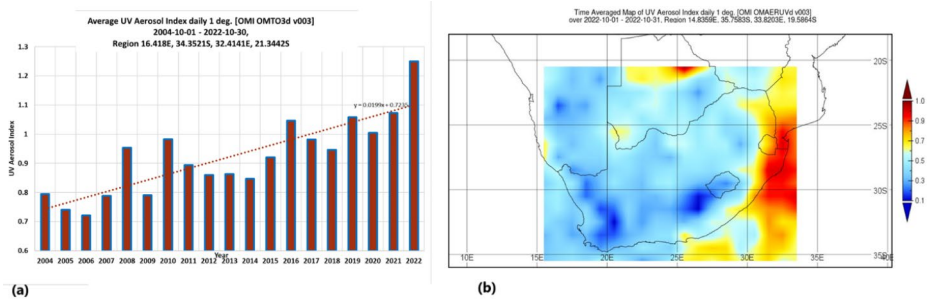


**Fig. 15** A time series (**a**) and map distribution (**b**) of the ultraviolet aerosol index (UVAI) area average over the study area from 2004 to 2022

This study also found that the heatwave led to elevated levels of low-level ozone and PM2.5, particularly in the Free State and North West provinces, reaching harmful levels for human health. Since 1971, the U.S. Environmental Protection Agency (EPA) has set national air quality standards for ozone at 80 parts per billion (ppb), averaged over 8 h. It is important to note that unhealthy ozone levels pose health risks, particularly on hot, sunny days. Even low levels of ozone can adversely affect health, especially in individuals with asthma, certain genetic conditions, the elderly, children, and outdoor workers exposed to these conditions for more than 8 h. Children, in particular, are vulnerable to ozone exposure due to their still-developing lungs. Additionally, black carbon concentrations and the ultraviolet aerosol index (UVAI) significantly increased, highlighting the poor air quality linked to the extreme weather.

The current study emphasizes the role of the Botswana subtropical high, coupled with the Angola heat low, in triggering long-lasting heat waves, as observed during the October 2022 drought. Other studies also recognize the importance of the Botswana High system over southern Africa, which is associated with a near-surface heat low and tropical warm air advection, focusing more on broader factors like ENSO (Mbokodo et al. 2023). A comparison of this study with previous research reveals that the heatwave event of October 2022 exhibited different weather patterns, linked to the southward expansion of the seasonal semi-stationary Angola heat low-pressure system. This led to an intensified trough, bringing dry, hot winds to the study area, in contrast to the omega-blocking pattern typically observed during summer heatwaves (e.g., Fazel-Rastgar and Sivakumar 2024). Also, the interaction between the Angola Low and Botswana High plays a crucial role in the atmospheric dynamics of Southern Africa. When these systems are strong, they suppress vertical mixing and reduce the height of the boundary layer, causing the air to stagnate near the surface. As a result, pollutants such as ozone and PM2.5 become trapped in the lower atmosphere, with limited vertical movement (Ranaivombola et al. 2024; Ncipha et al. 2020; Laban et al. 2018; Freiman and Piketh 2003; TYSON et al. 1996; Swap 1996). This leads to their accumulation, especially in urban areas, where concentrations can become dangerously high. Such stagnation negatively impacts air quality and poses a serious risk to public health. Understanding how these systems influence pollutant transport is essential for tackling regional air pollution challenges effectively.

Furthermore, this study highlights the need for better mitigation strategies to address the impacts of extreme heat events and air pollution, emphasizing the importance of improved

monitoring, early warning systems, and proactive measures for air quality and water resource management to reduce health and environmental risks.

The study's limitations include reliance on reanalysis data with limited resolution, which may affect the accuracy of localized findings. The study focuses on a single heatwave event, limiting the ability to draw conclusions about long-term climate trends. Additionally, gaps in air quality monitoring stations may have resulted in incomplete pollution data, and the study did not account for other contributing factors such as human activities, land use changes, or broader atmospheric influences. Future work could focus on long-term climate trends, improved air quality monitoring, and the impact of human activities and land use changes.

**Acknowledgements** Thanks are given to the NOAA/ESRL PSD, Physical Science Division, Boulder Colorado web page through http://www.esrl.noaa.gov/psd/, Giovanni online data system, developed and maintai ned by the NASA GES DISC and https://spei.csic.es/database.html for providing SPEI data. Also, thanks for obtaining the maximum and minimum observational data from Iowa State University of Science and Technology (https://mesonet.agron.iastate.edu/request/daily.phtml). Thanks to the South African Weather Service (SAWS) for providing data (https://www.weathersa.co.za/home/weatherques). The authors sincerely thank the editor, and reviewers for reviewing our manuscript and providing constructive feedback to improve our manuscript.

**Author contributions** FFR: Conceptualization; data curation; formal analysis; visualization; writing – original draft; methodology; investigation; supervision; project administration; writing, review and editing; software; validation. VS: Conceptualization, data curation, methodology, investigation, review and editing. MR: Conceptualization; data curation; formal analysis; methodology; investigation; review and editing; software; validation. BF: Conceptualization; validation; methodology; investigation, review and editing.

**Funding** Open access funding provided by University of KwaZulu-Natal.
Not applicable.

**Data availability** No datasets were generated or analysed during the current study.

## Declarations

**Ethics** Not applicable.

**Competing interests** The authors declare no competing interests.



## References

Abatzoglou JT, Williams AP (2016) Impact of anthropogenic climate change on wildfire across western US forests. Proc Nat Acad Sci 113(42):11770–11775. https://doi.org/10.1073/pnas.1607171113

Al Ameri ID, Briant RM, Engels S (2019) Drought severity and increased dust storm frequency in the middle East: A case study from the Tigris–Euphrates alluvial plain, central Iraq. Weather 74(12):416–426. https://doi.org/10.1002/wea.3445

Anderegg WR, Anderegg LD (2013) Hydraulic and carbohydrate changes in experimental drought-induced mortality of saplings in two conifer species. Tree Physiol 33(3):252–260. https://doi.org/10.1093/treephys/tpt016

Anderegg WR, Anderegg LD, Berry JA, Field CB (2014) Loss of whole-tree hydraulic conductance during severe drought and multiyear forest die-off. Oecologia 175(1):11–23. https://doi.org/10.1007/s00442-013-2875-5

Arnone E, Cucchi M, Gesso SD, Petitta M, Calmanti S (2020) Droughts prediction: A methodology based on climate seasonal forecasts. Water Resour Manage 34(14):4313–4328. https://doi.org/10.1007/s11269-020-02623-3

Attiya AA, Jones BG (2022) An extensive dust storm impact on air quality on 22 November 2018 in Sydney, Australia, using satellite remote sensing and ground data. Environ Monit Assess 194(6). https://doi.org/10.1007/s10661-022-10080-1

Attwood K, Washington R, Munday C (2024) The Southern African heat low: structure, seasonal and diurnal variability, and Climatological trends. J Clim 37(10):3037–3053. https://doi.org/10.1175/jcli-d-23-0522.1

Ceccherini G, Russo S, Ameztoy I, Marchese AF, Carmona-Moreno C (2017) Heat waves in Africa 1981–2015, observations and reanalysis. Nat Hazards Earth Syst Sci 17(1):115–125

CSIC (Spanish National Research Council). (n.d.). SPEIbase: The standardized precipitation-evapotranspiration index database. Retrieved February 7 (2025) from https://spei.csic.es/database.html

Demetillo MA, Anderson JF, Geddes JA, Yang X, Najacht EY, Herrera SA, Pusede SE (2019) Observing severe drought influences on Ozone air pollution in California. Environ Sci Technol 53(9):4695–4706. https://doi.org/10.1021/acs.est.8b04852

Dilley M, Heyman BN (1995) ENSO and disaster: droughts, floods and El Nino/Southern Oscillation warm events. Disasters 19(3):181–193. https://doi.org/10.1111/j.1467-7717.1995.tb00338.x

Driver P, Reason CJ (2017) Variability in the Botswana high and its relationships with rainfall and temperature characteristics over Southern Africa. Int J Climatol 37(S1):570–581. https://doi.org/10.1002/joc.5022

Ebi KL, Capon A, Berry P, Broderick C, De Dear R, Havenith G, Jay O (2021) Hot weather and heat extremes: health risks. Lancet 398(10301):698–708. https://doi.org/10.1016/s0140-6736(21)01208-3

Edwards B, Gray M, Hunter B (2014) The impact of drought on mental health in rural and regional Australia. Soc Indic Res 121(1):177–194. https://doi.org/10.1007/s11205-014-0638-2

Edwards B, Gray M, Hunter B (2018) The social and economic impacts of drought. Australian J Social Issues 54(1):22–31. https://doi.org/10.1002/ajs4.52

Falkner R, Buzan B (2022) Great powers, climate change, and global responsibilities: a concluding assessment. Great Powers Clim Change Global Environ Responsibilities, 278–289. https://doi.org/10.1093/oso/9780198866022.003.0013

Fazel-Rastgar F, Sivakumar V (2022) A severe weather system accompanied by a stratospheric intrusion during unusual warm winter in 2015 over the South Africa: an initial synoptic analysis. Remote Sens Applications: Soc Environ 28:100833. https://doi.org/10.1016/j.rsase.2022.100833

Fazel-Rastgar F, Sivakumar V (2023) A case study of weather impact on air pollution during the COVID-19 pandemic in South Africa. Sci Afr 22:e01914. https://doi.org/10.1016/j.sciaf.2023.e01914

Fazel-Rastgar F, Sivakumar V (2024) A case study on more recent heat wave occurred in South Africa, based on background weather synoptic and dynamic characteristics analysis. Bull Atmos Sci Technol 5:5. https://doi.org/10.1007/s42865-024-00068-9

Freiman MT, Piketh SJ (2003) Air transport into and out of the industrial highveld region of South Africa. J Appl Meteorol Climatology 42(7):994–1002

Ge H, Zeng G, Iyakaremye V, Yang X, Wang Z (2021) Comparison of atmospheric circulation anomalies between dry and wet extreme high-temperature days in the middle and lower reaches of the yellow river. Atmosphere 12(10):1265. https://doi.org/10.3390/atmos12101265

Greenwood S, Ruiz-Benito P, Martínez-Vilalta J, Lloret F, Kitzberger T, Allen CD, ... Jump AS (2017) Tree mortality across biomes is promoted by drought intensity, lower wood density and higher specific leaf area. Ecol Lett 20(4):539–553. https://doi.org/10.1111/ele.12748

Guan S, Wong DC, Gao Y, Zhang T, Pouliot G (2020) Impact of wildfire on particulate matter in the southeastern united States in November 2016. Sci Total Environ 724:138354. https://doi.org/10.1016/j.scitotenv.2020.138354

Iowa Environmental Mesonet. (n.d.). Daily summary data. Retrieved February 7 (2025) from https://mesonet.agron.iastate.edu/request/daily.phtml

Kalnay E, Kanamitsu M, Kistler R, Collins W, Deaven D, Gandin L, Iredell M, Saha S, White G, Woollen J, Zhu Y, Leetmaa A, Reynolds R, Chelliah M, Ebisuzaki W, Higgins W, Janowiak J, Mo KC, Ropelewski C, Joseph D (1996a) The NCEP/NCAR 40-Year reanalysis project. Bull Am Meteorol Soc 77(3):437–471. https://doi.org/10.1175/1520-0477(1996)077%3C0437:tnyrp%3E2.0.co;2

Kalnay E, Kanamitsu M, Kistler R, Collins W, Deaven D, Gandin L, Joseph D (1996b) The NCEP/NCAR 40-Year reanalysis project. Bull Am Meteorol Soc 77(3):437–471. https://doi.org/10.1175/1520-0477(1996)077%3C0437:tnyrp%3E2.0.co;2

Kapwata T, Gebreslasie MT, Wright CY (2022) An analysis of past and future heatwaves based on a heat-associated mortality threshold: towards a heat health warning system. Environ Health 21(1). https://doi.org/10.1186/s12940-022-00921-4

Laban TL, Van Zyl PG, Beukes JP, Vakkari V, Jaars K, Borduas-Dedekind N, Laakso L (2018) Seasonal influences on surface Ozone variability in continental South Africa and implications for air quality. Atmos Chem Phys 18(20):15491–15514

Lei Y, Yue X, Liao H, Zhang L, Zhou H, Tian C, Potosnak M (2022) Global perspective of drought impacts on Ozone pollution episodes. Environ Sci Technol 56(7):3932–3940. https://doi.org/10.1021/acs.est.1c07260

Llusià J, Peñuelas J, Gimeno B (2002) Seasonal and species-specific response of VOC emissions by mediterranean Woody plant to elevated Ozone concentrations. Atmos Environ 36(24):3931–3938. https://doi.org/10.1016/s1352-2310(02)00321-7

Lyon B (2009) Southern Africa summer drought and heat waves: observations and coupled model behavior. J Clim 22(22):6033–6046. https://doi.org/10.1175/2009jcli3101.1

Mbokodo I, Bopape M, Chikoore H, Engelbrecht F, Nethengwe N (2020) Heatwaves in the future warmer climate of South Africa. Atmosphere 11(7):712. https://doi.org/10.3390/atmos11070712

McClure CD, Jaffe DA (2018) US particulate matter air quality improves except in wildfire-prone areas. Proc Nat Acad Sci 115(31):7901–7906. https://doi.org/10.1073/pnas.1804353115

McTainsh G, Burgess R, Pitblado J (1989) Aridity, drought and dust storms in Australia (1960–84). J Arid Environ 16(1):11–22. https://doi.org/10.1016/s0140-1963(18)31042-5

McTainsh G, Chan Y, McGowan H, Leys, J., Tews K (2005) The 23rd October 2002 dust storm in Eastern Australia: characteristics and meteorological conditions. Atmos Environ 39(7):1227–1236. https://doi.org/10.1016/j.atmosenv.2004.10.016

Meque A, Pinto I, Maúre G, Beleza A (2022) Understanding the variability of heatwave characteristics in Southern Africa. Weather Clim Extremes 38:100498. https://doi.org/10.1016/j.wace.2022.100498

Mukherjee S, Ashfaq M, Mishra AK (2020) Compound drought and heatwaves at a global scale: the role of natural climate variability-associated synoptic patterns and land-surface energy budget anomalies. J Geophys Research: Atmos 125(11). https://doi.org/10.1029/2019jd031943

Munday C, Washington R (2017) Circulation controls on Southern African precipitation in coupled models: the role of the Angola low. J Geophys Research: Atmos 122(2):861–877. https://doi.org/10.1002/2016jd025736

Mwale D, Gan TY (2005) Wavelet analysis of variability, teleconnectivity, and predictability of the September–November East African rainfall. J Appl Meteorol Climatology 44(2):256–269

NASA Goddard Space Flight Center. (n.d.). Giovanni: The bridge between data and science. Retrieved February 7 (2025) from https://giovanni.gsfc.nasa.gov/giovanni/

Ncipha XG, Sivakumar V, Malahlela OE (2020) The influence of meteorology and air transport on CO2 atmospheric distribution over South Africa. Atmosphere 11(3):287

NOAA Physical Sciences Laboratory. (n.d.). Monthly/seasonal composites. Retrieved February 7 (2025) from https://psl.noaa.gov/cgi-bin/data/composites/printpage.pl

Nolte CG, Dolwick P, Fann N, Horowitz LW, Naik V, Pinder RW, Ziska LH (2018) Chapter 13: air quality. Impacts, risks, and adaptation in the United States: The fourth national climate assessment, volume II. https://doi.org/10.7930/nca4.2018.ch13

Odoulami RC, Abiodun BJ, Ajayi AE, Diasso UJ, Saley MM (2017) Potential impacts of forestation on heatwaves over West Africa in the future. Ecol Eng 102:546–556

Okello C, Githiora YW, Sithole S, Owuor MA (2024) Nature-based solutions for water resource management in Africa's arid and sem-arid lands (ASALs): A systematic review of existing interventions. Nature-Based Solutions 6:100172. https://doi.org/10.1016/j.nbsj.2024.100172

Onyeuwaoma N, Sivakumar V, Bade M (2024) Modelling drought in South Africa: meteorological insights and predictive parameters. Environ Monit Assess 196(10). https://doi.org/10.1007/s10661-024-13009-y

Paulo AA, Rosa RD, Pereira LS (2012) Climate trends and behavior of drought indices based on precipitation and evapotranspiration in Portugal. Nat Hazards Earth Syst Sci 12(5):1481–1491. https://doi.org/10.5194/nhess-12-1481-2012

Qian Z, Sun Y, Ma Q, Gu Y, Taichen, Feng P (2023) Understanding changes in heat waves, droughts, and compound events in Yangtze river valley and the corresponding atmospheric circulation patterns. https://doi.org/10.21203/rs.3.rs-2687144/v1

Qiu M, Ratledge N, Azevedo I, Diffenbaugh N, Burke M (2023) Drought impacts on the electricity system, emissions, and air quality in the Western US. https://doi.org/10.31223/x5zm1p

Ranaivombola M, Bègue N, Fazel-Rastgar F, Sivakumar V, Krysztofiak G, Berthet G, Bencherif H (2024) Characterization of AOD anomalies in September and October 2022 over Skukuza in South Africa. https://doi.org/10.5194/egusphere-2024-921

Richard Y, Fauchereau N, Poccard I, Rouault M, Trzaska S (2001) 20th century droughts in Southern Africa: Spatial and Temporal variability, teleconnections with oceanic and atmospheric conditions. Int J Climatol 21(7):873–885. https://doi.org/10.1002/joc.656

Rienecker MM, Suarez MJ, Gelaro R, Todling R, Bacmeister J, Liu E, Woollen J (2011) MERRA: NASA's modern-era retrospective analysis for research and applications. J Clim 24(14):3624–3648. https://doi.org/10.1175/jcli-d-11-00015.1

Russo S, Marchese AF, Sillmann J, Immé G (2016) When will unusual heat waves become normal in a warming Africa? Environ Res Lett 11(5):054016

Rustemeier E, Schneider U, Ziese M, Finger P, Becker A (2021) Updated gridded datasets version 2020 provided by the global precipitation climatology center (GPCC). https://doi.org/10.5194/egusphere-egu21-14611

Sankaran M (2019) Droughts and the ecological future of tropical savanna vegetation. J Ecol 107(4):1531–1549. https://doi.org/10.1111/1365-2745.13195

Schneider U, Ziese M, Meyer-Christoffer A, Finger P, Rustemeier E, Becker A (2016) The new portfolio of global precipitation data products of the global precipitation climatology center suitable to assess and quantify the global water cycle and resources. Proc Int Association Hydrol Sci 374:29–34

Schneider U, Finger P, Meyer-Christoffer A, Rustemeier E, Ziese M, Becker A (2017) Evaluating the hydrological cycle over land using the newly corrected precipitation climatology from the global precipitation climatology center (GPCC). Atmosphere 8(3):52. https://doi.org/10.3390/atmos8030052

Sivakumar MV, Hansen J (2007) Climate prediction and agriculture: advances and challenges. Springer Science & Business Media

Šmejkalová AH, Brzezina J (2022) The effect of drought on PM concentrations in the Czech Republic. Aerosol Air Qual Res 22(10):220130. https://doi.org/10.4209/aaqr.220130

Soulé PT (1992) Spatial patterns of drought frequency and duration in the contiguous USA based on multiple drought event definitions. Int J Climatol 12(1):11–24. https://doi.org/10.1002/joc.3370120103

South African Weather Service. (n.d.). Weather questions. South African Weather Service. Retrieved February 7 (2025) from https://www.weathersa.co.za/home/weatherques

Talley NJ, Stanley F, Lucas T, Horton R (2021) Health and climate change MJA–Lancet countdown report: Australia gets another failing grade in 2020 but shows signs of progress. Lancet 397(10287):e12–e14. https://doi.org/10.1016/s0140-6736(20)32632-5

Thomas K, Hardy RD, Lazrus H, Mendez M, Orlove B, Rivera-Collazo I, Winthrop R (2018) Explaining differential vulnerability to climate change: a social science review. WIREs Clim Change 10(2). https://doi.org/10.1002/wcc.565

Trentini L, Dal Gesso S, Venturini M, Guerrini F, Calmanti S, Petitta M (2022) A novel bias correction method for extreme events. Climate 11(1):3. https://doi.org/10.3390/cli11010003

Tyson PD, Garstang M, Kâllberg Swapr P, Edwards M (1996) An air transport climatology for subtropical Southern Africa. Int J Climatol 16(3):265–291. https://doi.org/10.1002/(sici)1097-0088(199603)16:3%3C265::aid-joc8%3E3.3.co;2-d

Vicente-Serrano SM, Beguería S, López-Moreno JI (2010) A multiscalar drought index sensitive to global warming: the standardized precipitation evapotranspiration index. J Clim 23(7):1696–1718. https://doi.org/10.1175/2009jcli2909.1

Vivaldo G, Masi E, Taiti C, Caldarelli G, Mancuso S (2017) The network of plants volatile organic compounds. Sci Rep 7(1). https://doi.org/10.1038/s41598-017-10975-x

Wang Y, Xie Y, Dong W, Ming Y, Wang J, Shen L (2017) Adverse effects of increasing drought on air quality via natural processes. Atmos Chem Phys 17(20):12827–12843. https://doi.org/10.5194/acp-17-12827-2017

Wang N, Du Y, Chen D, Meng H, Chen X, Zhou L, Yang F (2023) Spatial disparities of ozone pollution in the Sichuan basin spurred by an extreme heatwave. https://doi.org/10.5194/egusphere-2023-2284

Weckroth M, Ala-Mantila S (2022) Socioeconomic geography of climate change views in Europe. Glob Environ Change 72:102453. https://doi.org/10.1016/j.gloenvcha.2021.102453

Werner M, Vermooten S, Iglesias A, Maia R, Vogt J, Naumann G (2015) Developing a framework for drought forecasting and warning: Results of the DEWFORA project: M. Werner S. Vermooten. In: Drought: research and science-policy interfacing, pp 295–302. CRC Press

Yuan X, Wang L, Wood EF (2018) Anthropogenic intensification of Southern African flash droughts as exemplified by the 2015/16 season. Bull Am Meteorol Soc 99(1):S86–S90

Zhang F, Lei R, Zhai M, Pang X, Li N (2023) The impacts of anomalies in atmospheric circulations on Arctic sea ice outflow and sea ice conditions in the Barents and Greenland seas: case study in 2020. Cryosphere 17(11):4609–4628. https://doi.org/10.5194/tc-17-4609-2023

Zhao M, Running SW (2010) Drought-induced reduction in global terrestrial net primary production from 2000 through 2009. Science 329(5994):940–943. https://doi.org/10.1126/science.1192666